Received January 15, 2019, accepted February 5, 2019, date of publication February 22, 2019, date of current version March 12, 2019.

Digital Object Identifier 10.1109/ACCESS.2019.2900989

140-GHz TE_{340}-Mode Substrate Integrated Cavities-Fed Slot Antenna Array in LTCC

JUN XIAO, XIUPING LI, (Senior Member, IEEE), ZIHANG QI, (Student Member, IEEE), AND HUA ZHU, (Member, IEEE)

School of Electronic Engineering, Beijing University of Posts and Telecommunications, Beijing 100876, China
Beijing Key Laboratory of Work Safety Intelligent Monitoring, Beijing University of Posts and Telecommunications, Beijing 100876, China

Corresponding author: Xiuping Li (xpli@bupt.edu.cn)

This work was supported in part by the Equipment Development Department of the Central Military Commission under Project 6140518040116DZ02001, in part by the National Natural Science Foundation of China (NSFC) under Project 61601050, and in part by the National Science and Technology Major Project of China under Project 2017ZX03001028-003.

ABSTRACT In this paper, a TE_{340}-mode substrate-integrated cavity (SIC) excited 2 × 2 slot antenna subarray with two TE_{210}-mode SICs' loading is presented at 140 GHz in low-temperature co-fired ceramic. By using the TE_{340}-mode SIC, the number of vias used in the feeding network and the area of the feeding network can be reduced compared to the feeding network composed of conventional TE_{10}/TE_{20}-mode SIW power dividers. The proposed simplified and miniaturized high-order mode SIC-based feeding network leads to lower transmission loss and fabrication cost and reduces the fabrication difficulty. Each pair of radiating slots is loaded by a TE_{210}-mode SIC to improve the impedance bandwidth and the gain performance. For the proof of concept, an 8 × 8 antenna array is further designed and measured. The measured impedance bandwidth of the proposed 8 × 8 antenna array is 10.7% from 130.3 to 145 GHz for $|S_{11}| \leq -10$ dB. The measured peak gain is 20.5 dBi. The measured radiation efficiency is 59.2%.

INDEX TERMS 140 GHz, low temperature co-fired ceramic (LTCC), TE_{340} mode, TE_{210} mode, substrate integrated cavity (SIC), slot antenna.

I. INTRODUCTION

The D-band (110-170 GHz) has been allocated for the applications such as communications, radars, imaging [1]–[5]. High-level integrated antennas with excellent performance are highly desirable for these systems. A conventional high-gain or high-efficiency antenna is a parabolic reflector antenna or hollow waveguide based antenna. In [6], a parabolic reflector antenna is presented at 120 GHz with a peak gain of 48.7 dBi. However, the bulky size (antenna diameter is 450 mm) and large profile make it not suitable for integration with front-end planar circuits. In [7] and [8], a 32 × 32 and a 16 × 16 hollow waveguide based antenna arrays fabricated with a costly process called diffusion bonding are presented at D-band, respectively. These two arrays show the advantages of high gain (39.1 dBi and 31.7 dBi, respectively) and low profile (antenna array heights are 2.4 mm and 4.8 mm, respectively). However, high mechanical pressure in the fabrication process will deform the antennas especially when fabricating large and complex structures, which leads to a low rate of finished products. At such a high operating frequency band, the integration of high-performance antennas with front-end planar circuits is important and preferred. Low temperature co-fired ceramic (LTCC), a multilayer technology, can realize integration of passive/active devices with antennas in a package [9]–[12].

A planar waveguide structure named substrate integrated waveguide (SIW) [13] or laminated waveguide [14] has been widely used in antenna designs by many researchers because of its merits of low-loss characteristics, low fabrication costs and ease of integration. Millimeter-wave (MMW) antenna arrays based on SIW feeding networks have been realized with printed circuit board (PCB) and LTCC processes in much literature [15]–[19]. In [15] and [16], large arrays fed by TE_{10}-mode SIW feeding networks are presented with excellent performances. Compared to the dominant mode SIW, higher order mode SIW uses less metal vias which leads to lower loss and fabrication cost [17], [19]. In [17],

The associate editor coordinating the review of this manuscript and approving it for publication was Qingfeng Zhang.

a 140-GHz LTCC 8 × 8 slot array fed by a TE_{20}-mode SIW based feeding network is presented with a 15.3% bandwidth and a peak gain of 21.3 dBi. However, the seven-layer complicated feeding network occupies a relatively big area and leads to a low aperture efficiency (30%) and low radiation efficiency (35%). In [18], a LTCC-based low loss transmission line called ridge gap waveguide (GWG) forms a hybrid multilayer feeding network with an SIW feeding network for an 8 × 8 antenna array at W-band. The antenna array based on GWG feeding network shows higher gain and higher radiation efficiency compared to the array fed by SIW feeding network. However, a small air gap is required in the GWG structures which needs high machining accuracy in MMW bands and increases the fabrication difficulty.

In order to design a simplified and compact antenna array with better radiation performances, high-order mode substrates integrated cavities (SICs) have been introduced to the feeding networks of the antenna arrays [20], [21]. Compared to the conventional TE_{10}/TE_{20} mode SIW power divider based feeding network, less vias are used in the high-order mode SICs which simplifies and miniaturizes the feeding network of the antenna array leading to lower loss caused by feeding network and lower fabrication cost.

In this paper, high order mode (TE_{340} mode) SICs are designed to simplify the feeding network of a multilayer 8 × 8 antenna array in LTCC. Only four substrate layers are used in the proposed feeding network. Compared to the effective radiating aperture size of the 140-GHz LTCC 8 × 8 antenna array fed by TE_{20}-mode SIW based feeding network in [17] (15.1 mm × 10.8 mm), the effective radiating aperture size of the proposed 140-GHz LTCC 8× 8 antenna array (9.6 mm × 8.6 mm) has been reduced by 49.4%. Meanwhile, due to the simplified design and smaller occupied area of the feeding network, the measured aperture efficiency (51.1%) and radiation efficiency (59.2%) are higher than those in [17]. TE_{210}-mode SICs are loaded atop of the 8 × 8 slot array to improve the impedance matching and gain. The simulated and measured results show that the proposed array has the characteristics of wide bandwidth, high gain and stable radiation patterns, which indicates that the proposed array is a good candidate for 140-GHz wireless communications.

The paper is organized as follows. Section II presents the geometry of the 2 × 2 subarray. The design of the 8 × 8 array is illustrated in Section III. Section IV gives the measured results of the 8 × 8 array, and a conclusion is given in Section V. All simulations are performed using the full-wave electromagnetic simulator CST MWS.

II. 2 × 2 SUBARRAY

The geometry of the proposed 2 × 2 subarray is shown in Fig. 1. The multilayer LTCC substrates used in this paper are Ferro A6M with a dielectric constant of 5.9 and a loss tangent of 0.002. Each fired substrate layer thickness is 0.096 mm. The conductor used for the metallization and via is silver with a conductivity of $6.3\times10^7 s/m$ and a metallization thickness is 0.01 mm. There are six substrate layers and four

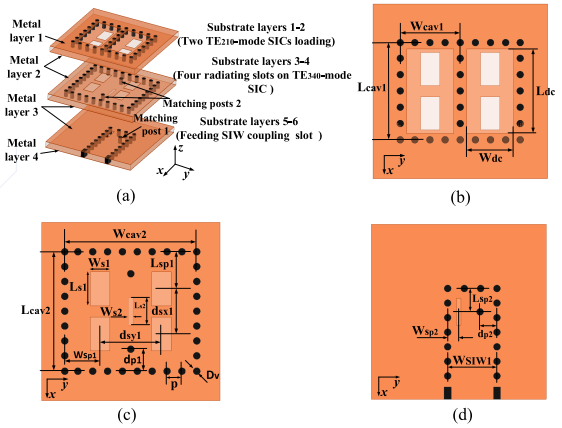

FIGURE 1. Geometry of the proposed antenna element. (a) Exploded view. (b) Top view of the TE_{210}-mode SICs. (c) Top view of the radiating element. (d) Top view of the feeding SIW.

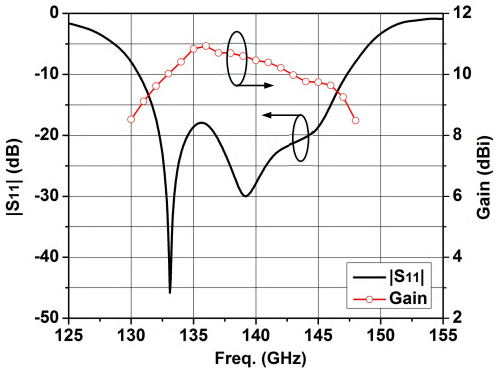

FIGURE 2. Simulated results of the 2 × 2 subarray.

metal layers in the 2 × 2 subarray as defined in Fig. 1. The 2 × 2 subarray consists of two open-ended TE_{210}-mode SICs loading, 2 × 2 radiating slots etched on the metal layer 2, a TE_{340}-mode feeding SIC, and a feeding SIW. The SICs loading improves the impedance matching and the gain of the slot antenna and the similar designs have been presented in [16] and [17]. The simulated results of the 2 × 2 subarray are shown in Fig. 2. The impedance bandwidth ($|S_{11}| \leq -10$dB) of the 2 × 2 subarray is 11.95% from 130.6 to 147.2 GHz. The simulated peak gain is 10.93 dBi at 136 GHz, and the gain is larger than 8.5 dBi within the impedance bandwidth. The simulated radiation patterns of the 2 × 2 subarray are shown in Fig. 3. The cross-polarization levels in both E (yoz)- and H (xoz)-planes are better than −36 dB. The optimized dimensions of the 2 × 2 subarray are listed in TABLE 1.

Fig. 4(a) shows the E-field distribution of TE_{340} mode inside the SIC in substrate layers 3-4 at 140 GHz. Fig. 4(b) shows that the four radiating slots etched on metal layer 2 have the same phase of the E-field which guarantees the 2 × 2 subarray good performance. The TE_{340}-mode SIC of the 2 × 2 subarray can be regarded as a four-way power divider. Compared to the conventional TE_{10}-mode SIW feeding network, the proposed TE_{340}-mode SIC design reduces the number of vias and simplifies the antenna structure.

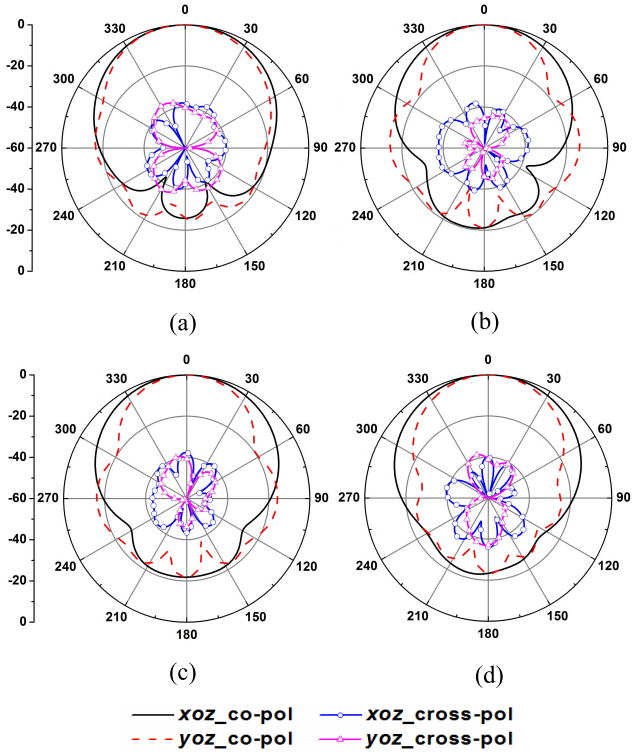

FIGURE 3. Simulated radiation patterns of the 2 × 2 subarray. (a) 131 GHz. (b) 135 GHz. (c) 140 GHz. (d) 147 GHz.

TABLE 1. Optimized dimensions of the 2 × 2 subarray (unit:mm).

Para.	L_{cav1}	W_{cav1}	L_{dc}	W_{dc}	L_{cav2}	W_{cav2}	L_{s1}
Values	1.67	1.03	1.45	0.81	2.01	2.22	0.57
Para.	W_{s1}	L_{s2}	W_{s2}	L_{sp1}	W_{sp1}	d_{sx1}	d_{sy1}
Values	0.33	0.46	0.08	0.625	0.595	0.76	1.03
Para.	d_{p1}	p	D_v	L_{sp2}	W_{sp2}	d_{p2}	W_{SIW1}
Values	0.37	0.25	0.12	0.4	0.19	0.29	0.845

Thus, the proposed high order TE_{340}-mode SIC leads to lower fabrication cost and lower transmission loss due to the feeding network. The E-field distributions inside the top two loaded SICs at 140 GHz are shown in Fig. 4(c). It can be seen that TE_{210} modes are excited inside these two loaded SICs.

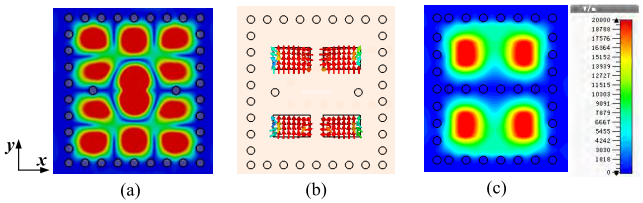

FIGURE 4. *E*-field distributions at 140 GHz. (a) Inside the TE_{340}-mode SIC in substrate layers 3-4. (b) On the 2 × 2 radiating slots on the metal layer 2. (c) Inside the two TE_{210}-mode SICs in substrate layers 1-2.

Three referenced antennas are designed for comparisons, as shown in Fig. 5. The total sizes of the three referenced antennas and the proposed 2 × 2 array are all 3.5 mm × 3 mm. In referenced antenna 1, two layers of Ferro A6M substrate are loaded atop of a TE_{10}-mode SIW 2 × 2 slot array as shown in Fig. 5(a). In referenced antenna 2,

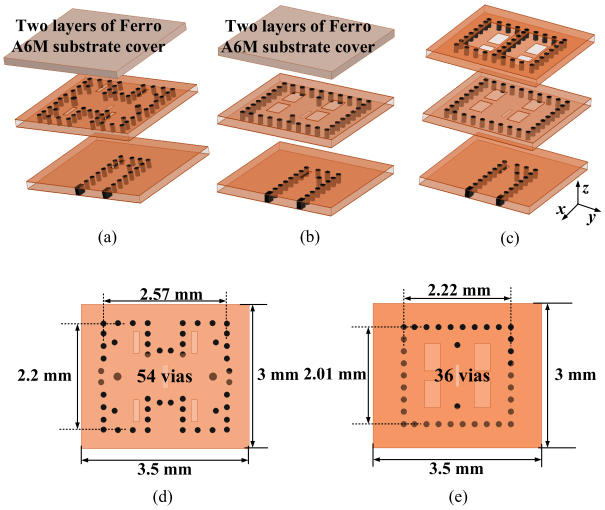

FIGURE 5. Three referenced antennas. (a) Referenced antenna 1: TE_{10}-mode SIW slot antenna with two layers of Ferro A6M substrate cover. (b) Referenced antenna 2: TE_{340}-mode SIC slot antenna with two layers of Ferro A6M substrate cover. (c) Referenced antenna 3: antenna removed the matching posts from the TE_{340}-mode SIC of the proposed 2 × 2 subarray. (d) TE_{10}-mode SIW feeding network in substrate layers of 3-4. (e) Proposed TE_{340}-mode SIC feeding network in substrate layers of 3-4.

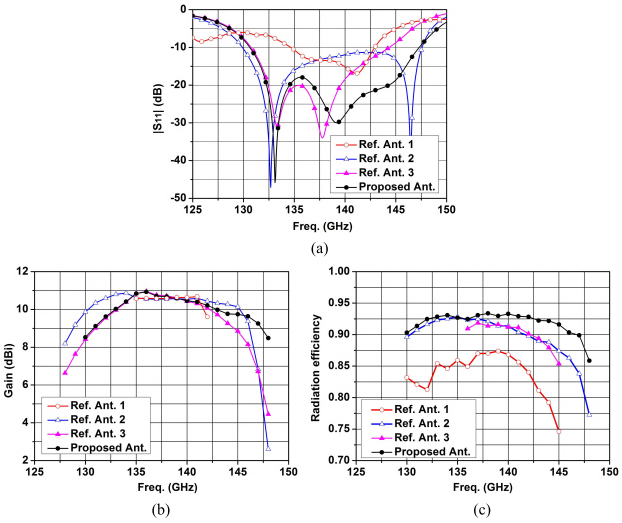

FIGURE 6. Simulated results of the three referenced antennas and the proposed 2 × 2 antenna array. (a) $|S_{11}|$. (b) Gains. (c) Radiation efficiencies.

two layers of Ferro A6M substrate are loaded atop of a TE_{340}-mode SIC 2 × 2 slot array as shown in Fig. 5(b). All the dimensions of the feeding network in referenced antenna 2 have the same values with those in the proposed 2 × 2 subarray. In referenced antenna 3, the two matching posts inside the TE_{340}-mode SIC are removed from the proposed 2 × 2 subarray as shown in Fig. 5(c). The simulated results of the three referenced antennas and the proposed 2 × 2 subarray are shown in Fig. 6. The impedance bandwidth ($|S_{11}| \leq -10$ dB) of the referenced antennas 1, 2 and 3 are 5.9% (134.7-142.9 GHz), 12.8% (129.9-147.6 GHz) and 9.9% (130.7-144.3 GHz), respectively. The peak gains of the referenced antennas 1, 2 and 3 are 10.7 dBi, 10.7 dBi and 10.95 dBi, respectively. It can be seen that the impedance

matching gets better by adopting TE_{340}-mode SIC feeding network and TE_{210}-mode SICs loading. The two matching posts in the TE_{340}-mode SIC of the proposed 2 × 2 subarray improve the impedance matching at higher frequencies (higher than 139 GHz). The TE_{10}-mode SIW feeding network and the proposed TE_{340}-mode SIC feeding network are shown in Figs. 5(d) and (e), respectively. The sizes of the two feeding networks are 2.57 mm × 2.2 mm and 2.22 mm × 2.01 mm, respectively. Miniaturized feeding network has been achieved by adopting high order mode SIC. The numbers of the vias in the TE_{10}-mode SIW feeding network and the TE_{340}-mode SIC feeding network are 54 and 36, respectively. 33% reduction in vias numbers has been achieved by using high order mode SIC which leads to lower fabrication cost. The radiation efficiencies of the four antennas are shown in Fig. 6(c). The radiation efficiencies of the three TE_{340}-mode SIC based antennas are higher than that of the TE_{10}-mode SIW based array within the operating bandwidth. It is noted that the only difference between referenced antennas 1 and 2 is the feeding networks in substrate layers of 3-4. It can be concluded that the TE_{340}-mode SIC feeding network has lower insertion loss compared to the TE_{10}-mode SIW feeding network.

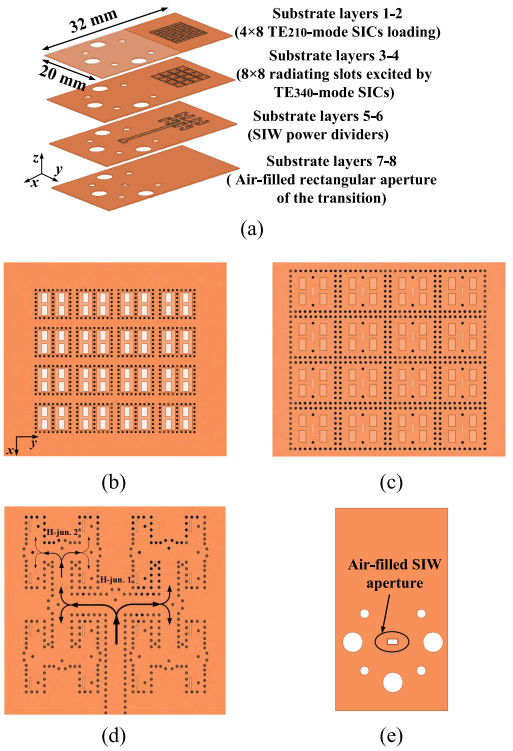

FIGURE 7. Geometry of the 8 × 8 antenna array. (a) 3-D exploded view of the 8 × 8 antenna array. (b) Top view of the 4 × 8 TE_{210}-mode SICs loading (substrate layers 1-2). (c) Top view of the 8 × 8 radiating slots excited by TE_{340}-mode SICs (substrate layers 3-4). (d) Top view of the SIW power divider (substrate layers 5-6). (e) Top view of the air-filled feeding aperture (substrate layers 7-8).

III. 8 × 8 ANTENNA ARRAY

Using the 2 × 2 subarray described above, an 8 × 8 antenna array is designed as shown in Fig. 7. The spacings between adjacent subarray along x- and y-directions are 2.26 mm (1.032 λ_0) and 2.47 mm (1.128 λ_0), respectively, where λ_0 is the wavelength at 137 GHz in free space. There are two types of H-junctions in the SIW power divider of the 8 × 8 antenna array, as shown in Fig. 7(d). The performances of these two H-junctions are crucial to the overall reflection coefficient performance of the 8 × 8 antenna array. The simulated models of these two H-junctions are shown in Fig. 8 and the simulated results are shown in Fig. 9. The impedance bandwidth ($|S_{11}| \leq -15$ dB) of the H-junction 1 and H-junction 2 are 18.5% (123.4-148.6 GHz) and 17.8% (124.2-148.4 GHz), respectively. Detailed dimensions of the two H-junctions are given in TABLE 2. For the purpose of measurement, a metallic waveguide WR-6 to SIW transition is designed. As shown in Fig. 10, the transition has a bandwidth from 130.7 to 146.5 GHz for $|S_{11}| \leq -20$ dB and an insertion loss of less than 0.4 dB in the operating band.

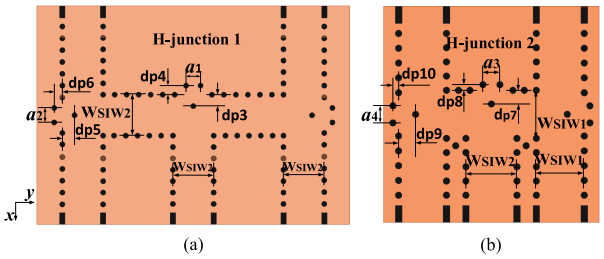

FIGURE 8. Geometry of two types of H-junctions in the SIW power divider. (a) H-junction 1. (b) H-junction 2.

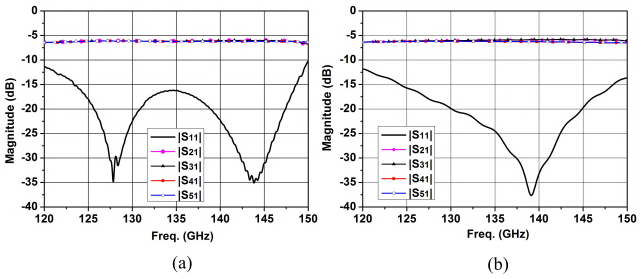

FIGURE 9. Simulated results of the two H-junctions. (a) H-junction 1. (b) H-junction 2.

TABLE 2. Detailed dimensions of the H-Junctions 1 and 2 (unit: mm).

Para.	a_1	a_2	dp_3	dp_4	dp_5	dp_6	W_{SIW2}
Values	0.32	0.32	0.25	0.2	0.27	0.18	0.9
Para.	a_3	a_4	dp_7	dp_8	dp_9	dp_{10}	
Values	0.3	0.3	0.24	0.1	0.3	0.1	

IV. EXPERIMENTS AND DISCUSSIONS

The proposed 8 × 8 antenna array is fabricated using the LTCC process. The photograph of the fabricated 8 × 8 antenna array is shown in Fig. 11(a). The overall size of the fabricated antenna array is 32 mm × 20 mm × 0.818 mm. The size of the effective radiating aperture is 9.6 mm × 8.6 mm. The simulated and measured $|S_{11}|$ and gains of the 8 × 8 antenna array are shown in Fig. 12. The simulated and measured bandwidth ($|S_{11}| \leq -10$ dB) are 11.4% from

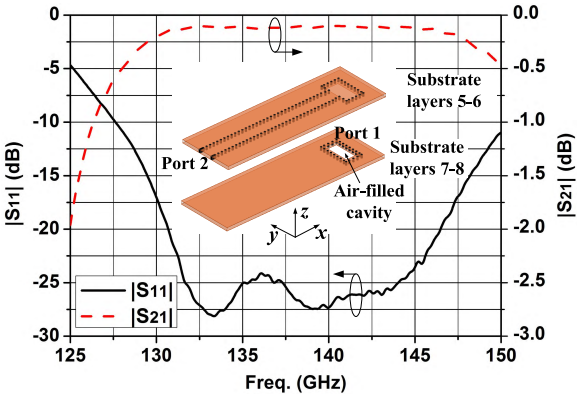

FIGURE 10. Simulated results of the proposed WR-6 waveguide to SIW transition.

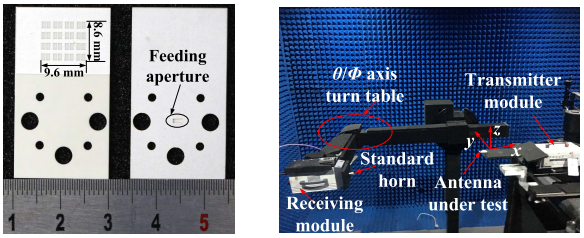

FIGURE 11. (a) Photograph of the fabricated 8 × 8 antenna array (left: top view, right: bottom view). (b) The fabricated 8 × 8 antenna array under test.

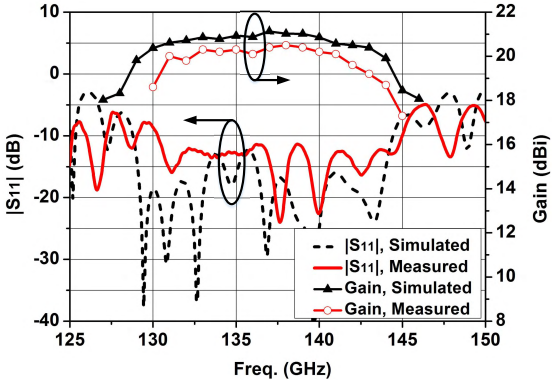

FIGURE 12. Simulated and measured $|S_{11}|$ and gains of the 8 × 8 antenna array.

128.8 to 144.4 GHz and 10.7% from 130.3 to 145 GHz, respectively. The simulated and measured peak gains of the 8 × 8 antenna array are 21.1 dBi at 137 GHz and 20.5 dBi at 138 GHz, respectively. The simulated radiation efficiency of the antenna array is above 61% within the bandwidth. The simulated peak radiation efficiency of the antenna array is 68% at 139 GHz. The measured radiation efficiency can be calculated by comparing the simulated directivity and the measured gain. Then the measured radiation efficiency of the antenna array is 59.2% at 138 GHz. The aperture area of the 8 × 8 antenna array is defined as 9.6 mm × 8.6 mm. The aperture efficiency, η, can be calculated by the following equation [22]

$$\eta = \frac{G\lambda^2}{4\pi S} \tag{1}$$

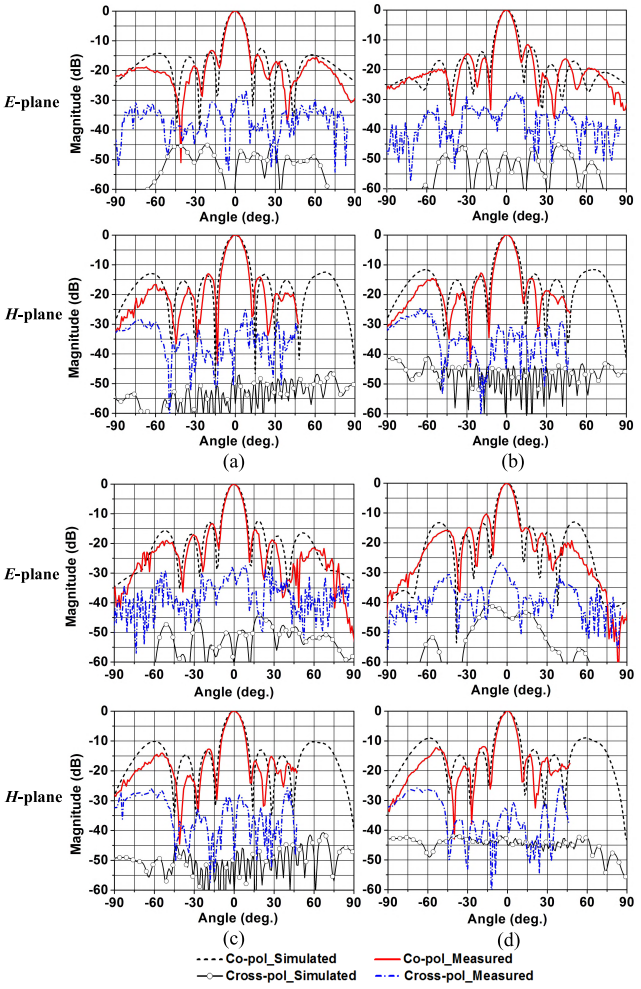

FIGURE 13. Simulated and measured radiation patterns for the proposed 8 × 8 antenna array. (a) 131 GHz. (b) 135 GHz. (c) 140 GHz. (d) 144 GHz.

where G and S are the measured gain and the effective radiating aperture of the antenna, respectively. Then, the aperture efficiency of the 8 × 8 antenna array can be calculated as 51.1% at 138 GHz.

The comparisons of the simulated and measured radiation patterns in E (yoz)- and H (xoz)-planes are shown in Fig. 13 for frequencies are 131, 135, 140, and 144 GHz. Due to the limitations of the measurement facilities, only the radiation patterns from −90° to 50° in the xoz-plane are obtained. Broadside and stable radiation patterns are observed. The measured first sidelobe levels of the radiation patterns are lower than −10.5 dB. The discrepancy between the measured and simulated first sidelobe levels is mainly resulted from the fabrication tolerance and the influence of the feeding setup near the antenna in measurement. The measured cross-polarization levels are lower than −25 dB within the bandwidth in both planes. Grating lobes which degrade the antenna efficiency and gain can be observed in the radiation patterns especially in the H-planes due to the large spacings between two adjacent subarrays. The spacings along x- and y- directions between two 2 × 2 subarrays can be reduced by making them share one row of via fence.

TABLE 3. Comparison between the proposed and reported millimeter-wave antenna arrays.

Ref.	Type	No. of Elements	Effective Radiating Aperture Size (mm)	Thickness (mm)	BW (GHz)	Gain (dBi)	Aperture Efficiency	Radiation Efficiency
[7]	Hollow-waveguide slot array (Diffusion bonding)	32×32	67.2 × 67.2 28.34λ × 28.34λ	2.4 1.01λ	119-134 (12%)	39.1	78.7%	80%
[8]	Planar plate array (Diffusion bonding)	16×16	34.3 × 34.3 15.83λ × 15.83λ	4.8 2.22λ	128-149 (15.1%)	31.7	43.1%	83%
[11]	Grid antenna array (LTCC)	240	12×12* 5.68λ × 5.68λ	0.48 0.23λ	137-147 (7%), $\|S_{11}\| \leq -5$ dB	17.6	n.a.	65%**
[15]	SIW-fed cavity-backed patch array (PCB)	8×8	30.4 × 34* 6.34λ × 7.1λ	4.1 0.86λ	58.2-67 (14.1%)	26	86%	68.5%
[16]	SIW slot array (LTCC)	4×4	23 × 20* 11.1λ × 9.63λ	0.76 0.37λ	130.2-158.8 (19.8%)	16.3	n.a.	55%**
[17]	TE_{20}-mode SIW slot array with SICs loading (LTCC)	8×8	15.1×10.8 6.91λ × 4.94λ	1.1 0.5λ	126.8-147.8 (15.3%)	21.3	30%	35%
[18]	SIC array with SIW feeding network (LTCC)	8×8	21.6 × 21.6* 6.72λ × 6.72λ	1.536 0.48λ	87-101 (14.9%)	22.9	34.3%	n.a.
[18]	SIC array with GWG & SIW hybrid feeding network(LTCC)	8×8	21.6 × 21.6* 6.72λ × 6.72λ	1.248 0.39λ	87-101 (14.9%)	23.8	42.3%	n.a.
[21]	GWG TE_{220}-mode slot array (PCB)	8×8	21.3 × 21.3 6.5λ × 6.5λ	1.11 0.34λ	82-102 (22.3%)	25.3	64%	n.a.
This Work	**TE_{340}-mode SICs slot array with SICs loading (LTCC)**	**8×8**	**9.6×8.6 4.41λ× 3.95λ**	**0.818 0.38λ**	**130.3-145 (10.7%)**	**20.5**	**51.1%**	**59.2%**

* Total size
** Simulated results

Structural characteristics and performances of different kinds of 140-GHz antenna arrays are listed in Table 3 for a comparison with our work. It can be seen that the proposed 8 × 8 array has the smallest effective radiating aperture electrical size (4.41λ × 3.95λ × 0.38λ) among those 8 × 8 millimeter-wave arrays due to the use of TE_{340}-mode SICs based feeding network. Compared to the 32 × 32 array in [7] and the 16 × 16 array in [8], it can be inferred that larger arrays expanded from the proposed 8 × 8 array will achieve smaller effective radiating aperture electrical size. It is observed that the proposed design features the advantages of compact size, high gain, and high efficiency among the millimeter-wave LTCC antenna arrays.

V. CONCLUSION

A TE_{340}-mode SICs based 8 × 8 slot antenna array with TE_{210}-mode SICs loading has been presented at 140 GHz. The proposed 8 × 8 antenna array is composed of sixteen 2 × 2 subarrays. 2 × 2 radiating slots in each subarray are fed by a TE_{340}-mode SIC. The simplified and miniaturized feeding TE_{340}-mode SICs not only reduce the feeding network loss but also reduce the fabrication cost. 4 × 8 TE_{210}-mode SICs are loaded atop of the 8 × 8 radiating slots to improve the performance of the array. It is demonstrated that the proposed antenna array can be a promising candidate for the *D*-band communication systems.

REFERENCES

[1] A. Hirata *et al.*, "120-GHz-band wireless link technologies for outdoor 10-Gbit/s data transmission," *IEEE Trans. Microw. Theory Techn.*, vol. 60, no. 3, pp. 881–895, Mar. 2012.
[2] X. Li and J. Yu, "Over 100 Gb/s ultrabroadband MIMO wireless signal delivery system at the D-band," *IEEE Photon. J.*, vol. 8, no. 5, Oct. 2016, Art. no. 7906210.
[3] T. Jaeschke, C. Bredendiek, S. Küppers, and N. Pohl, "High-precision D-band FMCW-radar sensor based on a wideband SiGe-transceiver MMIC," *IEEE Trans. Microw. Theory Techn.*, vol. 62, no. 12, pp. 3582–3597, Dec. 2014.
[4] M. Furqan, F. Ahmed, K. Aufinger, and A. Stelzer, "A D-band fully-differential quadrature FMCW radar transceiver with 11 dBm output power and a 3-dB 30-GHz bandwidth in SiGe BiCMOS," in *IEEE MTT-S Int. Microw. Symp. Dig.*, Jun. 2017, pp. 1404–1407.
[5] Z. Shen, N. Ito, E. Sakata, C. W. Domier, N. C. Luhmann, and A. Mase, "D-band double dipole antenna for use in millimeter wave imaging systems," in *Proc. IEEE Antennas Propag. Soc. Int. Symp.*, Jun. 2007, pp. 2658–2661.
[6] A. Hirata *et al.*, "120-GHz-band millimeter-wave photonic wireless link for 10-Gb/s data transmission," *IEEE Trans. Microw. Theory Techn.*, vol. 54, no. 5, pp. 1937–1944, May 2006.
[7] D. Kim, J. Hirokawa, M. Ando, J. Takeuchi, and A. Hirata, "64×64-element and 32×32-element slot array antennas using double-layer hollow-waveguide corporate-feed in the 120 GHz band," *IEEE Trans. Antennas Propag.*, vol. 62, no. 3, pp. 1507–1512, Mar. 2014.
[8] M. M. Zhou and Y. J. Cheng, "D-band high-gain circular-polarized plate array antenna," *IEEE Trans. Antennas Propag.*, vol. 66, no. 3, pp. 1280–1287, Mar. 2018.
[9] J.-H. Lee, N. Kidera, G. DeJean, S. Pinel, J. Laskar, and M. M. Tentzeris, "A *V*-band front-end with 3-D integrated cavity filters/duplexers and antenna in LTCC technologies," *IEEE Trans. Microw. Theory Techn.*, vol. 54, no. 7, pp. 2925–2936, Jul. 2006.
[10] M. Sun, Y. P. Zhang, D. Liu, K. M. Chua, and L. L. Wai, "A ball grid array package with a microstrip grid array antenna for a single-chip 60-GHz receiver," *IEEE Trans. Antennas Propag.*, vol. 59, no. 6, pp. 2134–2140, Jun. 2011.
[11] B. Zhang *et al.*, "Integration of a 140 GHz packaged LTCC grid array antenna with an InP detector," *IEEE Trans. Compon., Packag., Manuf. Technol.*, vol. 5, no. 8, pp. 1060–1068, Aug. 2015.
[12] A. D. Carlofelice, F. de Paulis, A. Fina, U. D. Marcantonio, A. Orlandi, and P. Tognolatti, "Compact and reliable T/R module prototype for advanced space active electronically steerable antenna in 3-D LTCC technology," *IEEE Trans. Microw. Theory Techn.*, vol. 66, no. 6, pp. 2746–2756, Jun. 2018.
[13] D. Deslandes and K. Wu, "Integrated microstrip and rectangular waveguide in planar form," *IEEE Microw. Wireless Compon. Lett.*, vol. 11, no. 2, pp. 68–70, Feb. 2001.
[14] H. Uchimura, T. Takenoshita, and M. Fujii, "Development of a 'laminated waveguide'," *IEEE Trans. Microw. Theory Techn.*, vol. 46, no. 12, pp. 2438–2443, Dec. 1998.
[15] Y. Li and K.-M. Luk, "60-GHz substrate integrated waveguide fed cavity-backed aperture-coupled microstrip patch antenna arrays," *IEEE Trans. Antennas Propag.*, vol. 63, no. 3, pp. 1075–1085, Mar. 2015.

[16] J. Xu, Z. N. Chen, X. Qing, and W. Hong, "140-GHz planar broadband LTCC SIW slot antenna array," *IEEE Trans. Antennas Propag.*, vol. 60, no. 6, pp. 3025–3028, Jun. 2012.
[17] J. Xu, Z. N. Chen, X. Qing, and W. Hong, "140-GHz TE_{20}-mode dielectric-loaded SIW slot antenna array in LTCC," *IEEE Trans. Antennas Propag.*, vol. 61, no. 4, pp. 1784–1793, Apr. 2013.
[18] B. Cao, H. Wang, Y. Huang, and J. Zheng, "High-gain L-probe excited substrate integrated cavity antenna array with LTCC-based gap waveguide feeding network for W-band application," *IEEE Trans. Antennas Propag.*, vol. 63, no. 12, pp. 5465–5474, Dec. 2015.
[19] Y. Kimura, J. Hirokawa, M. Ando, and N. Goto, "Frequency characteristics of alternating-phase single-layer slotted waveguide array with reduced narrow walls," in *Proc. IEEE Antennas Propag. Soc. Int. Symp.*, vol. 2, Jul. 1997, pp. 1450–1453.
[20] W. Han, F. Yang, J. Ouyang, and P. Yang, "Low-cost wideband and high-gain slotted cavity antenna using high-order modes for millimeter-wave application," *IEEE Trans. Antennas Propag.*, vol. 63, no. 11, pp. 4624–4631, Nov. 2015.
[21] B. Cao, H. Wang, and Y. Huang, "W-band high-gain TE_{220}-mode slot antenna array with gap waveguide feeding network," *IEEE Antennas Wireless Propag. Lett.*, vol. 15, pp. 988–991, 2015.
[22] J. Volakis, *Antenna Engineering Handbook*, 4th ed. New York, NY, USA: McGraw-Hill, 2007. [Online]. Available: https://mhebooklibrary.com/doi/book/10.1036/0071475745

JUN XIAO received the B.Eng. and M.Eng. degrees from the Harbin Institute of Technology, Harbin, China, in 2008 and 2011, respectively. He is currently pursuing the Ph.D. degree in electronic science and technology with the Beijing University of Posts and Telecommunications, Beijing, China. His research interests include UWB antennas, millimeter-wave antennas, and THz antennas.

XIUPING LI (M'05–SM'07) received the B.S. degree from Shandong University, in 1996, and the Ph.D. degree from the Beijing Institute of Technology, in 2001.

From 2001 to 2003, she was a Research Fellow with Nanyang Technological University, Singapore. In 2003, she was a Research Professor with Yonsei University, Seoul, South Korea. Since 2004, she has been with the Beijing University of Posts and Telecommunications, as an Associate Professor, and was promoted to be a Professor, in 2009. She holds more than 20 PRC patents. She has authored four books and over 100 journal and conference papers. Her current research interests include millimeter-wave and THz antennas, RFID systems, and RF MMIC design. She has been selected in the New Century Excellent Talents Support Plan in the National Ministry of Education and in the Beijing Science and Technology Nova Support Plan, in 2007 and 2008, respectively. She received the Second Prize of Progress in Science and Technology from the Chinese Institute of Communications, in 2015. She was a recipient of the awards of Distinguished Youth Teacher of Beijing, in 2017, and Excellent Teacher of Beijing, in 2017.

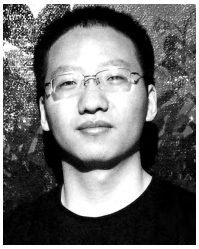

ZIHANG QI (S'17) received the B.E. degree, in 2013. He is currently pursuing the Ph.D. degree with the Beijing University of Posts and Telecommunications. His current research interests include millimeter-wave/THz antennas and microwave filters.

HUA ZHU (M'17) received the M.S. degree from the Guilin University of Electronic Technology, Guilin, China, in 2010, and the Ph.D. degree from the Beijing University of Posts and Telecommunications, Beijing, China, in 2015, where she is currently a Lecturer. Her research interests include UHF RFID beam scanning antenna array design in complex environment and millimeter-wave/terahertz antenna design.